Structural imaging in the Rocky Mountain Foothills (Alberta) using magnetotelluric exploration

Wen Xiao and Martyn Unsworth

ABSTRACT

The magnetotelluric method has improved significantly in recent years and is being used in hydrocarbon exploration in regions where seismic exploration is difficult. This includes areas where high-velocity carbonates and volcanic rocks are present in the near surface, overthrust belts, and in subsalt imaging. Magnetotelluric exploration was used in the Rocky Mountain Foothills in 2002 to determine if thrust-related structures could be imaged through the subsurface resistivity structure. Broadband magnetotelluric data were collected at 26 stations on a profile that extended southwest from Rocky Mountain House to the Front Ranges. Two-dimensional inversion was used to derive a resistivity model that was a compromise between fitting the magnetotelluric data and being spatially smooth. The resistivity model imaged the Alberta basin as a thick package of low-resistivity units that could be traced to the southwest where they form the footwall of the Brazeau thrust fault. The subsurface geometry in the magnetotelluric-derived resistivity model is in good agreement with well-log data and a coincident seismic section. Zones of low resistivity in the underthrust rocks may be caused by fracture-enhanced porosity associated with anticlines and fault-bend folds.

INTRODUCTION

Seismic reflection is a highly effective tool for imaging complex structures in hydrocarbon exploration. However, in certain scenarios, seismic data quality can be severely diminished. For example, near-surface carbonates and volcanic rocks can degrade the quality

Manuscript received December 18, 2004; provisional acceptance April 14, 2005; revised manuscript received July 21, 2005; final acceptance October 15, 2005.
DOI:10.1306/10150504140

AUTHORS

Wen Xiao ~ *Institute of Geophysical Research, Department of Physics, University of Alberta, Edmonton, Alberta, Canada, T6G 2J1; wxiao@phys.ualberta.ca*

Wen Xiao received his B.Sc. degree in 1993 in geology from the Northwest University at Xian in the People's Republic of China. From 1993 to 2000, he worked as a hydrocarbon exploration researcher for Sichuan Petroleum Research Institute. He moved to Canada in 2001 and completed his M.Sc. degree in geophysics in the Department of Physics at the University of Alberta in 2004.

Martyn Unsworth ~ *Institute of Geophysical Research, Department of Physics, University of Alberta, Edmonton, Alberta, Canada, T6G 2J1; unsworth@phys.ualberta.ca*

Martyn Unsworth is currently a professor at the University of Alberta. He received both his B.A. degree in natural sciences (1986) and his Ph.D. in earth sciences (1991) from Cambridge University. Following 2 years of postdoctoral research at the University of British Columbia, he was a research professor at the University of Washington in Seattle from 1993 to 2000. Since 2000, he has been on the faculty of the University of Alberta, and his research is focused on electromagnetic exploration methods. This includes applications in continental tectonics, with recent studies of the San Andreas fault, the Tibetan Plateau, and the Canadian Cordillera. He has also applied electromagnetic methods to environmental and exploration studies.

ACKNOWLEDGEMENTS

This project was funded by research grants to Martyn Unsworth from the Natural Science and Engineering Research Council, the Canadian Foundation for Innovation, the Alberta Science and Research Investments Program, the Alberta Ingenuity Fund, and the University of Alberta. Additional magnetotelluric instrumentation and technical support were provided by Phoenix Geophysics. Seismic data were provided by Husky Energy. Field assistance from Di Qingyun, Natalia Gomez, Damien Meilleux, Flora Paganelli, Shah Shareef, Wolfgang Soyer, and Alex Walcott is acknowledged. Discussions with John Waldron and Richard Kellett are gratefully acknowledged. Reviews by David Pivnik, Jim Rogers, Joseph Studlick, and editor Ernest Mancini greatly improved the manuscript.

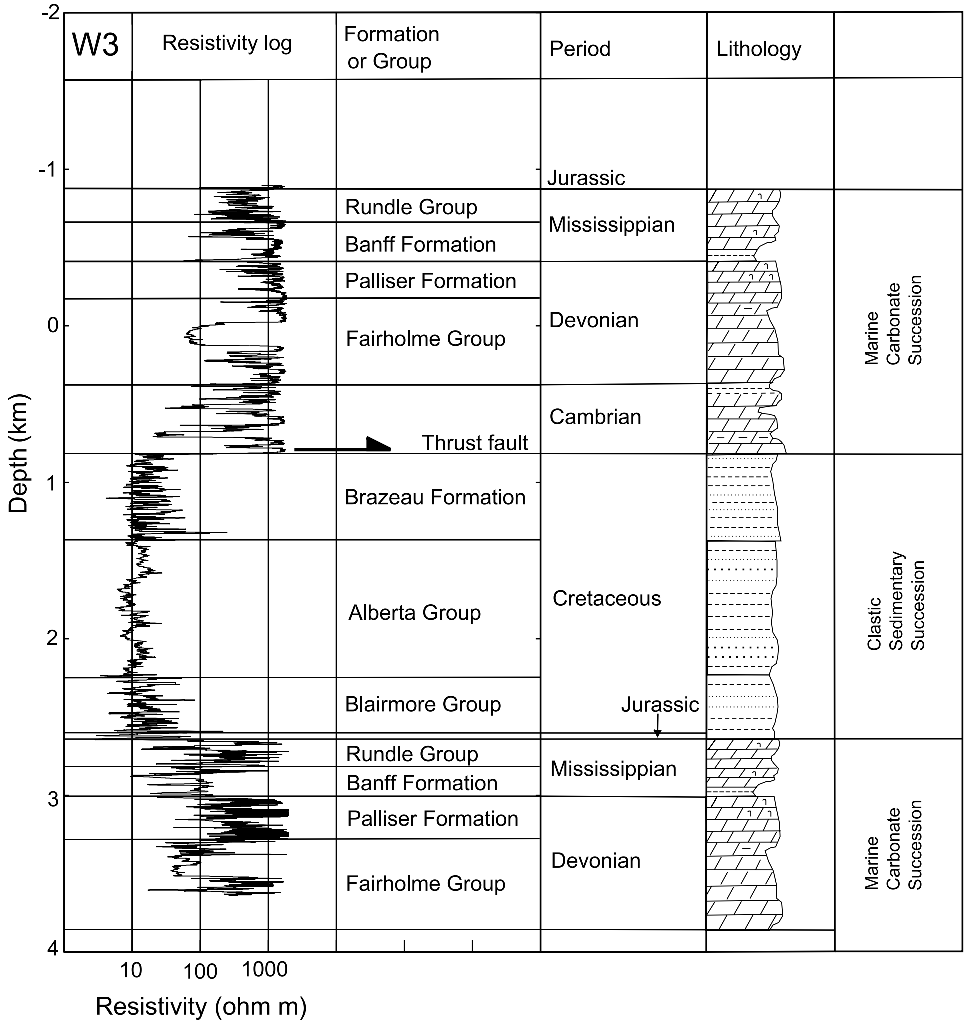

Figure 1. Resistivity log for well W3 (00/05-13-037-12w500). The depth is below mean sea level. Location of the well is shown in Figure 3. Stratigraphic column for the study area is based on Lawton et al. (1996).

of seismic data through static effects. Problems can also arise in overthrust belts, where high-velocity rocks are emplaced over a low-velocity layer. In these situations, other geophysical methods, such as gravity, magnetics, and magnetotellurics, can be used to provide alternative or complementary information about the subsurface structure.

The Rocky Mountain Foothills is a major overthrust belt and is the focus of ongoing hydrocarbon exploration in western Canada. Seismic exploration has been very successful, but some of the imaging problems listed above have been encountered. Paleozoic carbonate rocks exposed at the surface can yield poor-quality seismic data, and high-velocity carbonate thrust sheets can complicate imaging at depth. This geometry commonly results in a high-electrical-resistivity thrust sheet emplaced above a low-resistivity footwall and is favorable for magnetotelluric exploration (Bedrosian et al., 2001; Park et al., 2003). This situation is commonly found in the Rocky Mountain Foothills (Figure 1).

At this location, the Brazeau thrust fault has placed Paleozoic rocks over Mesozoic clastic sedimentary rocks. The formation resistivity of the Mesozoic strata is about 10 ohm m, whereas the overlying Paleozoic strata have a resistivity in the range 100–1000 ohm m. This strong resistivity contrast suggests that structural imaging with electromagnetic data could be feasible in this setting, as suggested by Densmore (1970).

Remote sensing of electrical resistivity in the upper few kilometers can be accomplished with controlled source electromagnetic methods and has been used in shallow surveys in the Rocky Mountain Foothills (Duckworth, 1983). However, for deeper exploration and simpler field logistics, the natural source magnetotelluric method is more suitable. The magnetotelluric method was developed in the 1950s (Tikhonov, 1950; Cagniard, 1953) but was not immediately useful for hydrocarbon exploration. Prior to the 1990s, magnetotelluric data were used primarily to provide regional maps of depth to basement and sediment thickness in basins where seismic data were of poor quality. The wide station spacing and unrealistic one-dimensional (1-D) interpretation restricted the application to regions where other types of geophysical data were ambiguous. Since the early 1990s, the improvement in field acquisition with multiple receivers and small station spacing has combined with dramatic increases in data processing and numerical modeling to make magnetotellurics a viable technique for hydrocarbon exploration in regions with a distinct resistivity contrast. Several case studies have shown the utility of the magnetotelluric method in this context (Christopherson, 1991; Watts and Pince, 1998). In this article, a case study is presented, which shows that modern magnetotelluric exploration can reliably image the detailed geometry of underthrust packages of sedimentary rock and can perhaps be useful in identifying zones of elevated permeability and porosity.

GEOLOGICAL SETTING OF THE SOUTHERN CENTRAL ROCKY MOUNTAIN FOOTHILLS

The Rocky Mountain Foothills in Alberta are located between the Western Canada sedimentary basin and the Rocky Mountains (Figure 2). The Paleozoic section is composed mainly of marine carbonate sediments, whereas clastic sedimentary rocks, such as shales, siltstones, and sandstones, dominate the Mesozoic section (Lawton et al., 1996) (Figure 1). The western margin of North America underwent extension from the Proterozoic to the Triassic and compressive deformation from the Middle Jurassic to the Eocene caused by terrane accretion (Monger and Price, 1979). Compressive tectonics resulted in the shortening of the western margin of the Western Canada sedimentary basin and formed the Rocky Mountains and Foothills (Wright et al., 1994). Structures

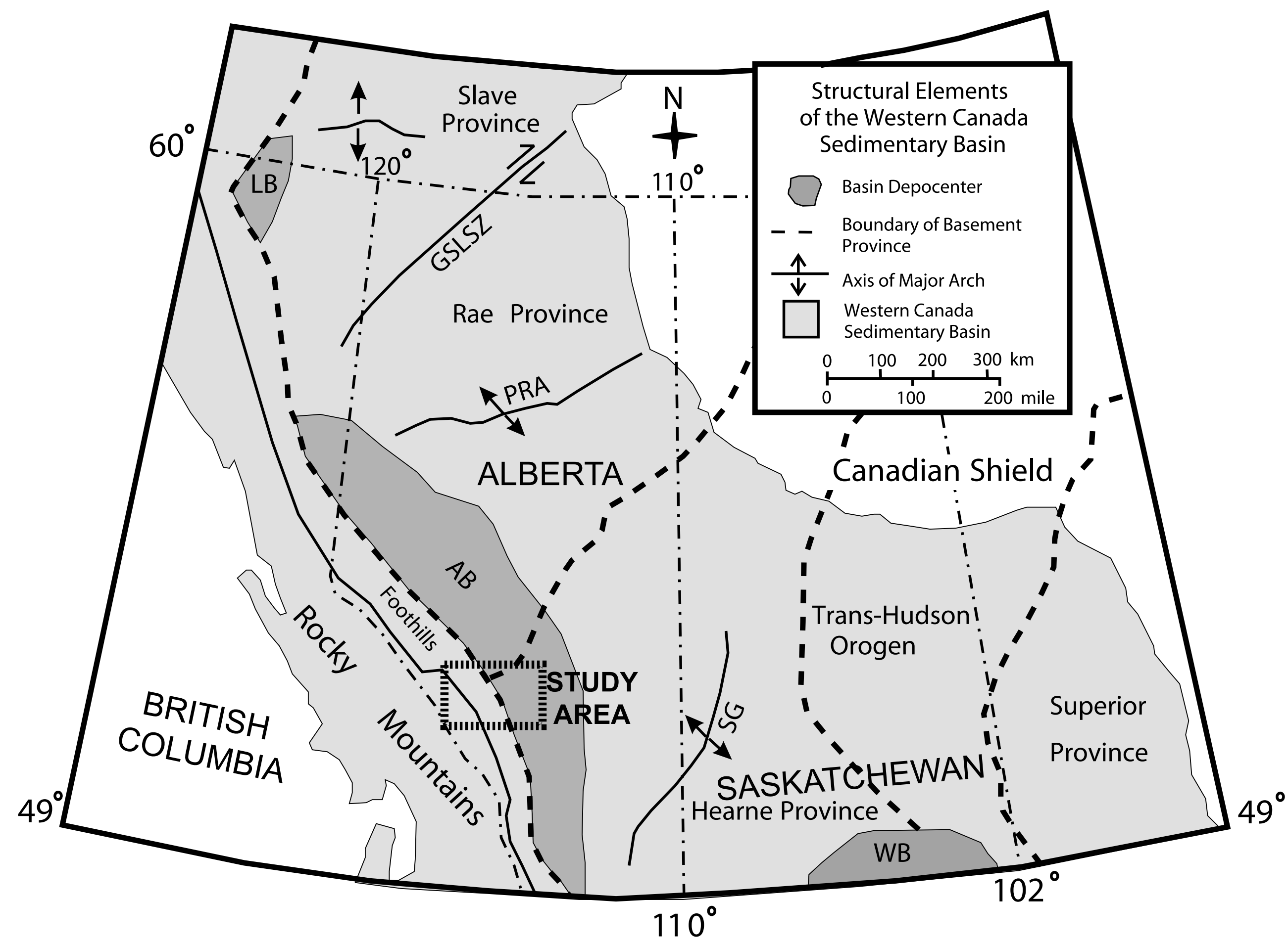

Figure 2. The structural elements of the Western Canada sedimentary basin. GSLSZ = Great Slave Lake shear zone, PRA = Peace River Arch, SG = Sweet Grass Bow Island Arch, LB = Liard basin, WB = Williston basin, AB = Alberta basin. The magnetotelluric profile described in this study is located in the box.

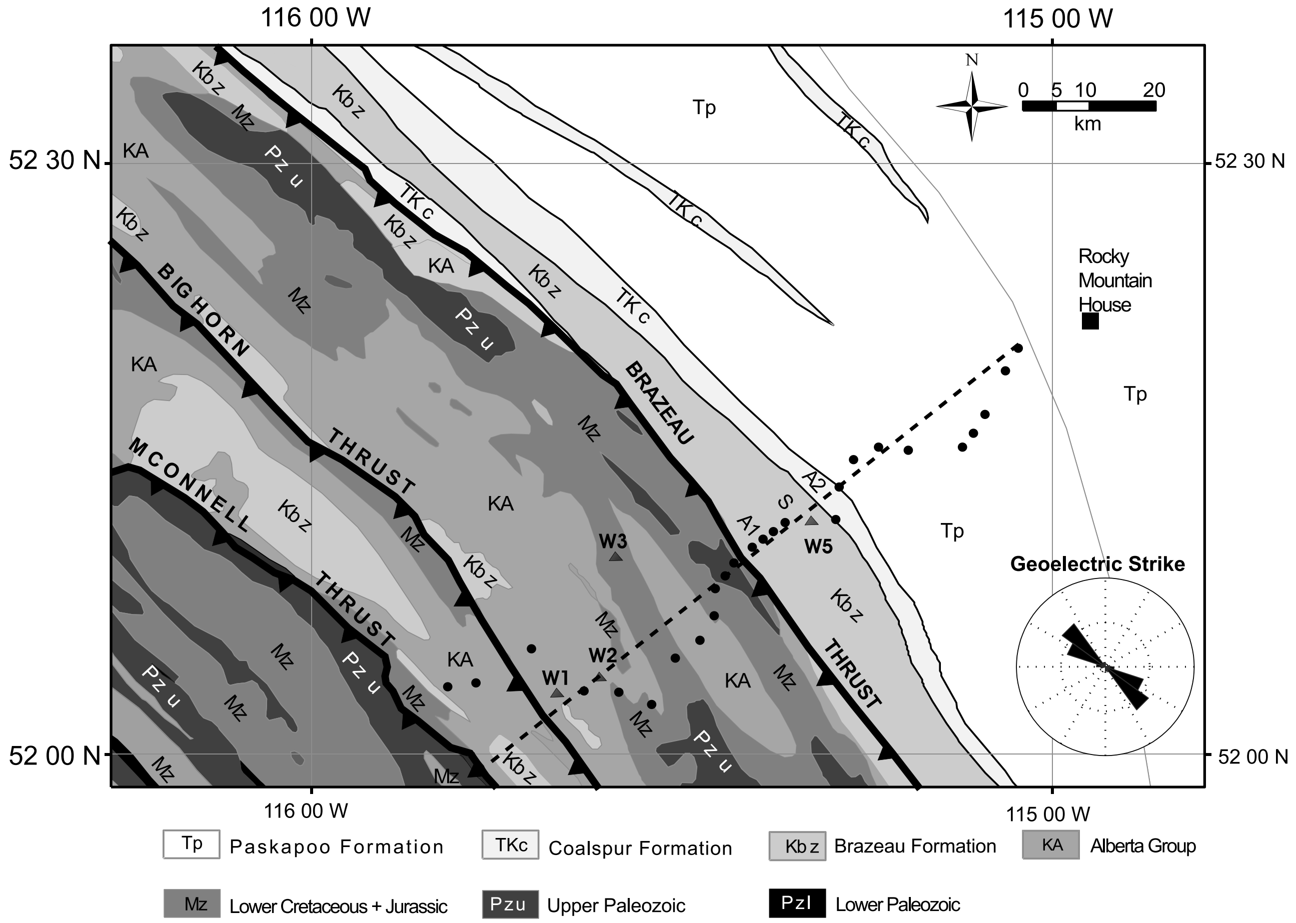

Figure 3. Geological map showing the location of magnetotelluric sites (circles) and well logs used in the study. Triangles show the locations of wells in Figures 4 and 7. The rose diagram shows the regional geoelectric strike (frequency band: 100–0.01 Hz) determined by tensor decomposition. The dashed line is the profile onto which magnetotelluric stations were projected for 2-D analysis. Geological map is modified from the geological map of Alberta, Alberta Geological Survey/Alberta Energy and Utility Board (1999).

in the Foothills are generally complex, and different structural styles have developed because of variations in lithology. A change in structural style from thrust dominated in the south to fold dominated in the north is generally observed. This is associated with a northward increase in the shale content of the Devonian and Mississippian section. This results in a northward decrease in the competency of the entire Phanerozoic sedimentary sequence in the Rocky Mountain Foothills (Wright et al., 1994) and perhaps a decrease in bulk electrical resistivity. A triangle zone occurs at the eastern limit of deformation along most of the southern Rocky Mountain Foothills (Jones, 1982).

In the study area, the dominant thrust fault is the Brazeau thrust, which has carried Cambrian rocks over Mesozoic rocks with a displacement of at least 20 km (12 mi) at the Paleozoic level (Langenberg et al., 2002) (Figure 3). The hanging wall of the Brazeau thrust fault contains an almost complete Paleozoic section about 1800 m (5905 ft) thick, and the underthrust Mesozoic section is interpreted to extend more than 10 km (6 mi) to the west in the footwall.

Figure 4a shows a seismic time section located close to the magnetotelluric profile discussed in this article. A simple geological interpretation based on well-log data and a gross velocity model is shown on the section. In this area, the Brazeau thrust fault climbs from the top of the Cambrian to the lower part of the Brazeau Formation, then moves horizontally about 12 km (7 mi), and finally reaches the surface on the west side of anticline A1. Shortening and accretion in the Brazeau Formation has formed the anticlines (A1 and A2) and a syncline (S).

EXPLANATION OF THE MAGNETOTELLURIC METHOD

The magnetotelluric method uses natural electromagnetic signals to image the subsurface resistivity structure. The signals originate in worldwide lightning activity and the Earth's magnetosphere. Magnetotelluric exploration works by recording time variations of the natural electric and magnetic fields at the Earth's surface. If the measured electric and magnetic fields are E_x and H_y, then the apparent resistivity of the Earth is given by

$$\rho_{xy} = \frac{1}{2\pi f \mu_0} \left| \frac{E_x}{H_y} \right|^2 \qquad (1)$$

where f is the frequency of the signal, and μ_0 is a constant (Vozoff, 1991). The electromagnetic signals penetrate a distance into the Earth that is termed the ''skin depth'' (δ), which is defined in meters as

$$\delta = 503\sqrt{\frac{\rho}{f}} \qquad (2)$$

It can be seen that measuring resistivity at greater depths requires lower frequencies. Subsurface electrical resistivity can range from 0.1 to 10,000 ohm m, and the frequencies used in magnetotelluric range from 1000 to 0.0001 Hz. Thus, the skin depth can range from tens of meters to hundreds of kilometers. The apparent resistivity represents the volume average of the Earth's electrical resistivity over a hemisphere with radius equal to the skin depth. A magnetotelluric phase angle can also be defined and is the phase shift between E_x and H_y at a given frequency. If the apparent resistivity increases with decreasing frequency, the phase will be less than 45°. Similarly, a decrease in apparent resistivity will correspond to a phase angle greater than 45°. The phase is generally more sensitive than apparent resistivity to changes in subsurface resistivity as a function of depth (Vozoff, 1991).

In more complex regions with two-dimensional (2-D) and three-dimensional (3-D) resistivity structure, different values of the apparent resistivity are derived from the electric and magnetic field components measured in different horizontal directions. The application of 1-D magnetotelluric data analysis in this situation will give misleading results, and most data sets require a 2-D or 3-D analysis. In a general 3-D environment, all six components of the electric and magnetic field are interdependent. However, in a 2-D Earth with the geological strike in the x-direction, this situation becomes simpler. Suppose E_x, E_y, and E_z are the electric fields in the x-, y-, and z-directions, and H_x, H_y, and H_z are the corresponding magnetic fields. Then it can be shown that E_x, H_y, and H_z are mutually dependent and are called the transverse electric mode (Vozoff, 1991). Apparent resistivity computed from E_x and H_y in the transverse electric mode is most sensitive to along-strike conductors. The H_x, E_y, and E_z field components comprise the transverse magnetic mode, with the apparent resistivity computed from E_y and H_x. In the transverse magnetic mode, electric current flows across the boundaries of different resistivities, which causes electric charges to build up on the interfaces. Thus, apparent resistivity computed from the transverse magnetic mode is more effective than that computed from the transverse electric mode in locating interfaces between regions of different resistivity. Significant progress has been made in the last decade in 3-D magnetotelluric modeling and inversion (Mackie et al., 1993). However, if just a single profile of magnetotelluric stations is available and 3-D effects can be shown to be small, then a 2-D analysis has many advantages.

In magnetotellurics, small-scale, near-surface structures can distort the electric fields and shift the apparent resistivity curves up or down. This effect is called static shift (Jones, 1988; Vozoff, 1991). It is routinely observed in field magnetotelluric data and can complicate its interpretation. If a 1-D analysis is used, the static shifts cannot be removed without external measurements of near-surface resistivity. In recent years, several techniques have been developed to compute the static shifts directly (Sternberg et al., 1988), to filter them (Torres-Verdin and Bostick, 1992), or to estimate them during inversion (deGroot-Hedlin, 1991). As a consequence, static shifts are a less serious problem in magnetotelluric data interpretation than before.

The magnetotelluric method is sometimes confused with magnetic exploration. It should be noted that magnetic surveys use absolute measurements of the magnetic field to determine variations of magnetic susceptibility. In contrast, magnetotelluric exploration uses time variations in the magnetic and electric field to determine electrical resistivity. By using multiple frequencies, magnetotellurics can reliably determine depth variations of the electrical resistivity. This gives it additional resolution compared to potential field methods such as magnetic and gravity exploration. However, the fact that electromagnetic signals diffuse in the Earth gives magnetotellurics a lower spatial

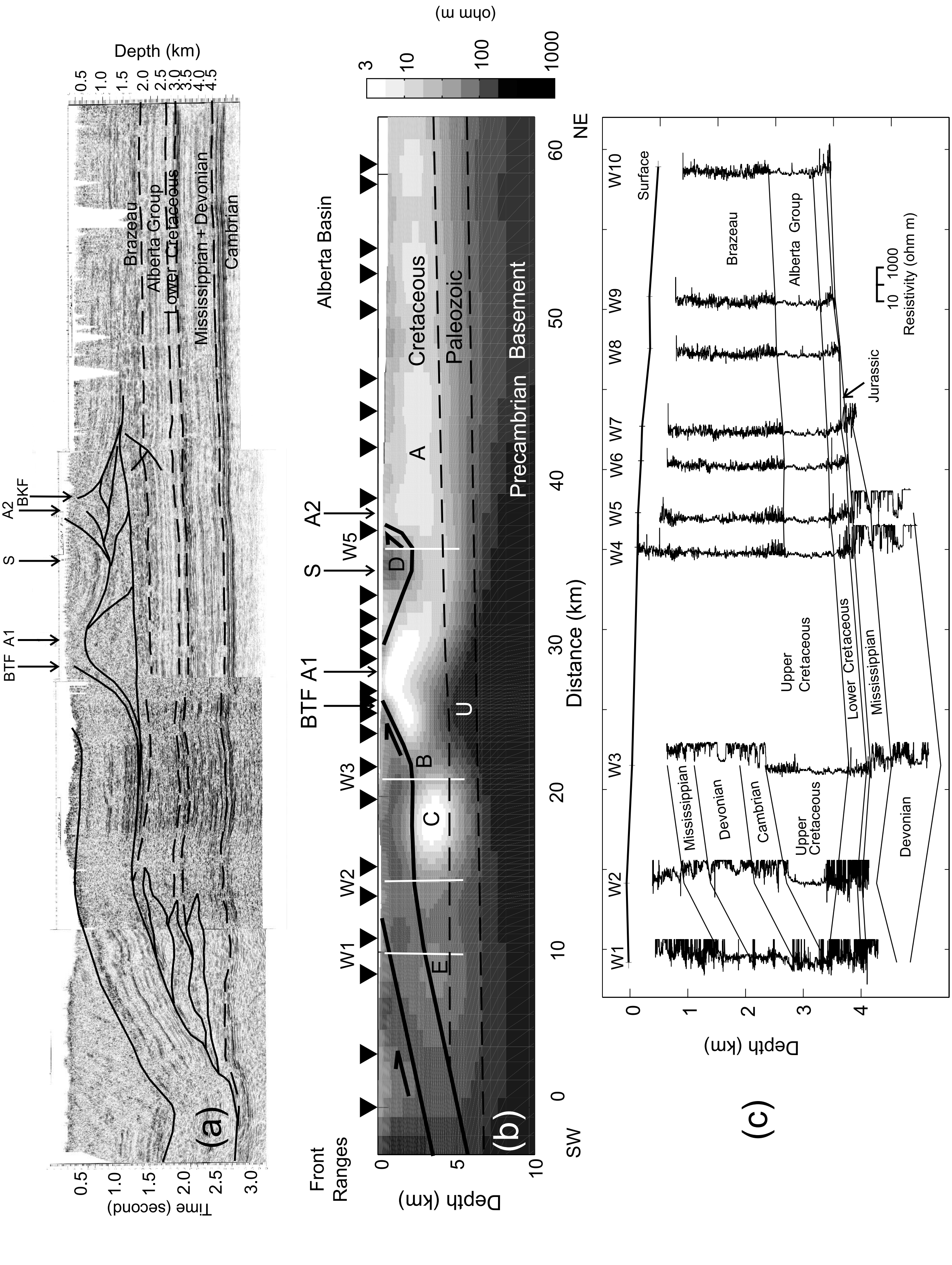
(a)
(b)
(c)
BTF
A1
S
A2
BKF
Time (second)
Depth (km)
Brazeau
Alberta Group
Lower Cretaceous
Mississippian + Devonian
Cambrian
Front Ranges
Alberta Basin
SW
NE
Cretaceous
Paleozoic
Precambrian Basement
Distance (km)
(ohm m)
W1
W2
W3
W4
W5
W6
W7
W8
W9
W10
Surface
Upper Cretaceous
Lower Cretaceous
Mississippian
Devonian
Cambrian
Jurassic
Resistivity (ohm m)

resolution than methods using wave propagation such as seismic reflection.

A review of the magnetotelluric technique can be found in Vozoff (1991) and Simpson and Bahr (2004). Some practical details of magnetotelluric data collection with commercial contractors are listed in the Appendix.

MAGNETOTELLURIC DATA COLLECTION, PROCESSING, AND INVERSION IN THE FOOTHILLS

To evaluate whether magnetotelluric data could effectively image thrust-related structures in the Rocky Mountain Foothills, a pilot survey was undertaken in 2002 by the University of Alberta. Magnetotelluric data were collected at 26 locations (Figure 3), and magnetotelluric data were recorded overnight using a Phoenix Geophysics V5-2000 system. The time-series data were processed to yield estimates of apparent resistivity and phase in the frequency band 100–0.001 Hz using the method of Jones and Jodicke (1984). This processing requires that a Fourier transform is taken of the electric and magnetic field variations, with many estimates obtained by analyzing different parts of the time series. These multiple estimates are then averaged to improve signal-to-noise in the data. A major improvement in the quality of magnetotelluric data has resulted from the application of robust statistics to the averaging process in recent years (Egbert, 1997). The time-series data processing used synchronous data recorded at two magnetotelluric stations. This allows local noise to be distinguished from the magnetotelluric signals through the remote reference technique (Gamble et al., 1979). Typical sources of noise in the 2002 survey included electric power lines, cathodically protected pipelines, and ground vibration.

Significant static shifts were observed at some stations near the Brazeau thrust and were corrected in two steps:

- From the high-frequency magnetotelluric data, the surface resistivity of Cretaceous strata east of the Brazeau thrust fault is about 20 ohm m. The hanging wall is composed of carbonates with a resistivity range from 100 to 200 ohm m. Thus, the apparent resistivity curves of the four stations were shifted down to the same order as the neighboring stations at the highest frequency.
- The automated 2-D magnetotelluric inversion algorithm was used to compute small static shift coefficients. By allowing the static shifts to be free parameters, the inversion solved simultaneously for the structure and static shifts, thus ensuring that structures appearing in the models were not simply caused by the incorrect removal of static shift coefficients.

The next important stage in magnetotelluric data analysis is to determine the dimensionality and strike direction of the magnetotelluric data. This is commonly done with tensor decomposition, a technique that separates the effect of regional-scale and small-scale structures in magnetotelluric data. Several computer algorithms have been developed, and this study used the algorithm of McNeice and Jones (2001). This determined a well-defined geoelectric strike of N30°W, which is consistent with the regional geological strike (Figure 3). Tensor decomposition also showed that the data are relatively 2-D, which justified the application of 2-D inversion to the data. The magnetotelluric data were then rotated into a N30°W coordinate frame and displayed as data pseudosections (Figure 5). Several features can be observed in the pseudosections:

1. Low resistivity values characterize the shallow structure of the Alberta basin (30–60 km; 18–37 mi), as indicated by the apparent resistivity above 1 Hz.
2. The apparent resistivity increases at frequencies below 1 Hz in the Alberta basin, indicating the presence of high-resistivity basement rocks.
3. Higher apparent resistivities are observed to the west of the Brazeau thrust fault (0–30 km; 0–18 mi).

Figure 4. Comparison of the magnetotelluric inversion model with well log and a seismic section located 1–2 km (0.6–1.2 mi) southeast. (a) Migrated seismic time section close to the magnetotelluric profile; BTF = Brazeau thrust fault; BKF = prominent backthrust fault; A1, A2 = anticlines; S = syncline. The depth in the seismic section was converted from time with the velocity model from Lawton et al. (1996). (b) Magnetotelluric inversion model with station locations shown with inverted triangles; A–E and U denote resistivity features observed in the magnetotelluric inversion model. (c) Well-log cross section; using data from the Alberta Energy and Utility Board (EUB). Geological divisions are based on Geowell General Well Standard Report from the EUB.

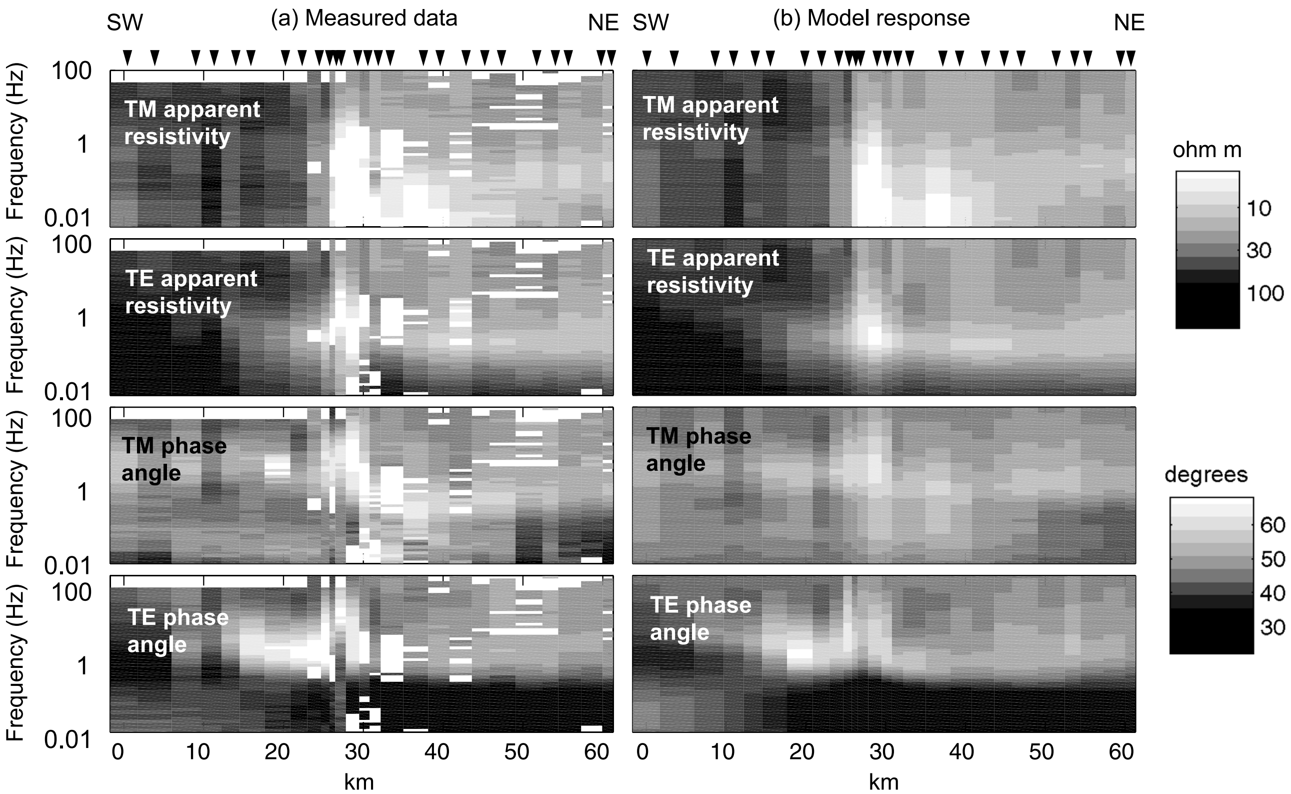

Figure 5. (a) Measured magnetotelluric data after static shift correction and rotation to N30°W coordinate system. White blocks denote noisy data that were excluded from the analysis. (b) Computed magnetotelluric response of the inversion model (Figure 4b). Note that a good fit is obtained between measured and computed data at most stations and frequencies.

4. A ridge of low resistivities in the transverse electric mode at 1 Hz west of the Brazeau thrust (10–25 km; 6–15 mi) indicates that a low resistivity layer is present at shallow depth.

Further interpretation of the magnetotelluric data requires that the frequency be converted to true depth and is analogous to converting time to depth in seismic data processing. This was achieved by the use of an automated inversion algorithm that yielded a 2-D resistivity model (Rodi and Mackie, 2001). This algorithm finds the smoothest resistivity model that fits the magnetotelluric data. It is appropriate for magnetotelluric data because it reflects the diffusive nature with which magnetotelluric signals travel in the Earth. A wide range of inversion parameters were used to ensure that the final model was well defined. The model in Figure 4b was obtained by inverting both transverse electric and transverse magnetic mode data over the frequency band of 100–0.01 Hz. The magnetotelluric data are fit to a root-mean-square error of 1.48, which indicates a statistically acceptable fit. Close agreement is achieved between the observed and predicted pseudosections (Figure 5).

Several distinct resistivity features (A–E) can be observed in Figure 4b:

A = 4–5-km (2.5–3.1-mi)-thick low-resistivity layer in the Alberta basin that can be traced west and dips west at the Brazeau thrust fault
B = a resistive break in feature A
C = pronounced zone of low resistivity at a 3–5-km (1.8–3.1 mi) depth
D = shallow high resistivity east of the triangle zone
E = zone of moderate resistivities at a 3–5-km (1.8–3.1 mi) depth northeast of the Front Ranges

It is important to verify that these model features are required to account for the measured magnetotelluric data. This requires that other competing models are considered, and the degree to which they also fit the magnetotelluric data is critically examined. This was undertaken by editing the model and observing how well the edited model fits the data. This analysis

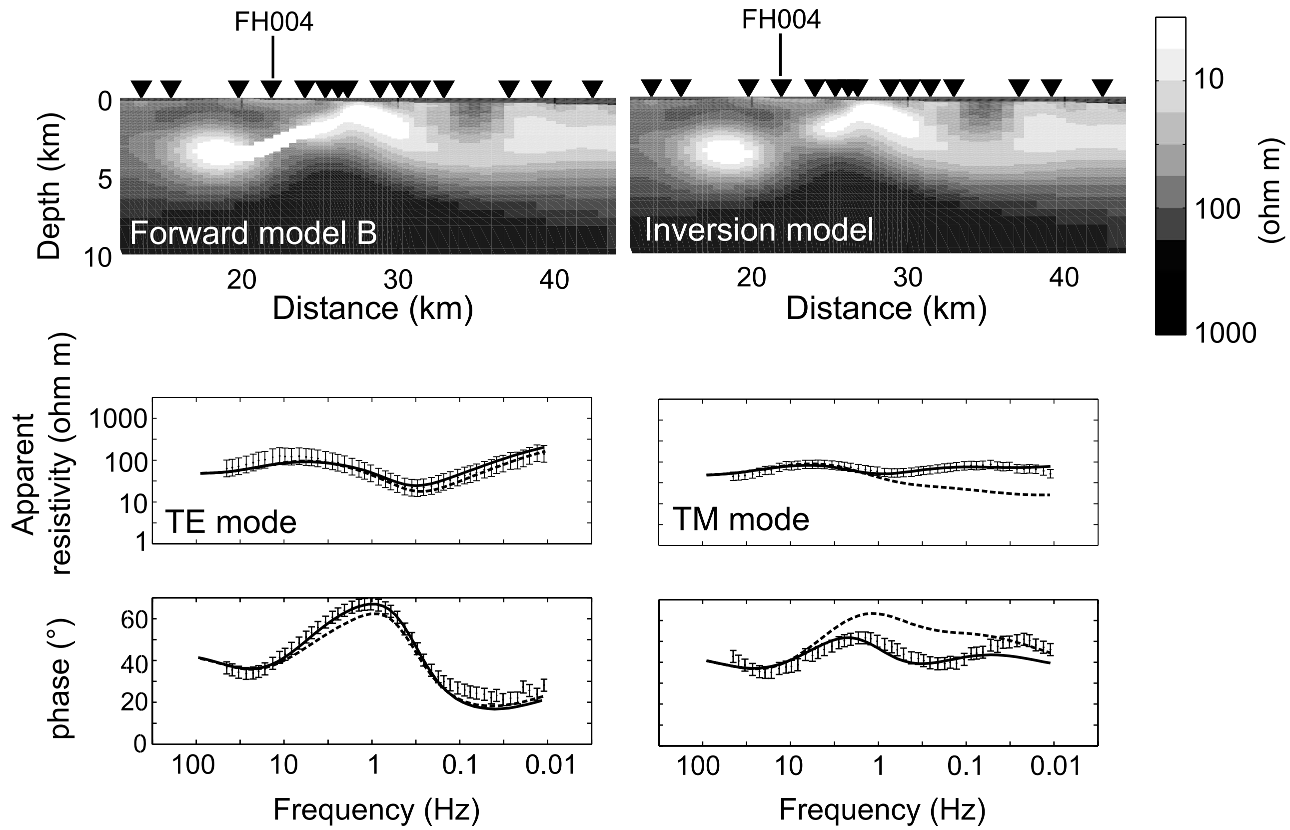

Figure 6. Test to determine if the feature B in Figure 4b is required to account for the measured magnetotelluric data. The right model shows the inversion result from Figure 4b. The left model shows an edited version with the gap B replaced with lower resistivity material to make the underthrust Cretaceous rocks uniform in resistivity. The magnetotelluric response at station FH004 of the original model fits the data (solid line). When the resistivity of the gap is decreased, the fit to the data is degraded significantly (dashed line). The normalized root-mean-square misfit increases from 1.49 to 2.73. This quantity should be in the range 1–1.5 to be acceptable.

showed that the features (B–E) were required by the magnetotelluric data. Results for feature B illustrate how this process is implemented (Figure 6). The reliability of the magnetotelluric inversion model is also examined through the synthetic inversions described below.

INTERPRETATION OF THE RESISTIVITY MODEL

Interpretation of the resistivity model used both the coincident seismic data and well-log information (Figures 4c, 7). A comparison of resistivity models and resistivity logs does not often give the type of agreement that is observed between seismic data and acoustic logs. This is primarily because magnetotelluric signals use long spatial wavelengths that average short spatial wavelength variations in electrical resistivity. In contrast, resistivity logs are obtained with an instrument that is much closer to the formation being studied. The agreement shown in Figure 7, and discussed below, is typical for that observed between these two independent measurements of subsurface resistivity.

Alberta Basin

Within the Alberta basin, the resistivity structure is dominated by a low-resistivity layer (A). From offsets 40–65 km (24–37 mi), this low-resistivity layer is located above the high-resistivity layer (100–1000 ohm m) that dips gently west. Layer A can be divided into (1) an upper 20–50-ohm-m layer that extends to a depth of 2 km (1.2 mi) and (2) and underlying 10-ohm-m layer at depths of 2–4 km (1.2–2.4 mi). This is consistent with the resistivity structure observed in well logs W4–W10 (Figure 4c).

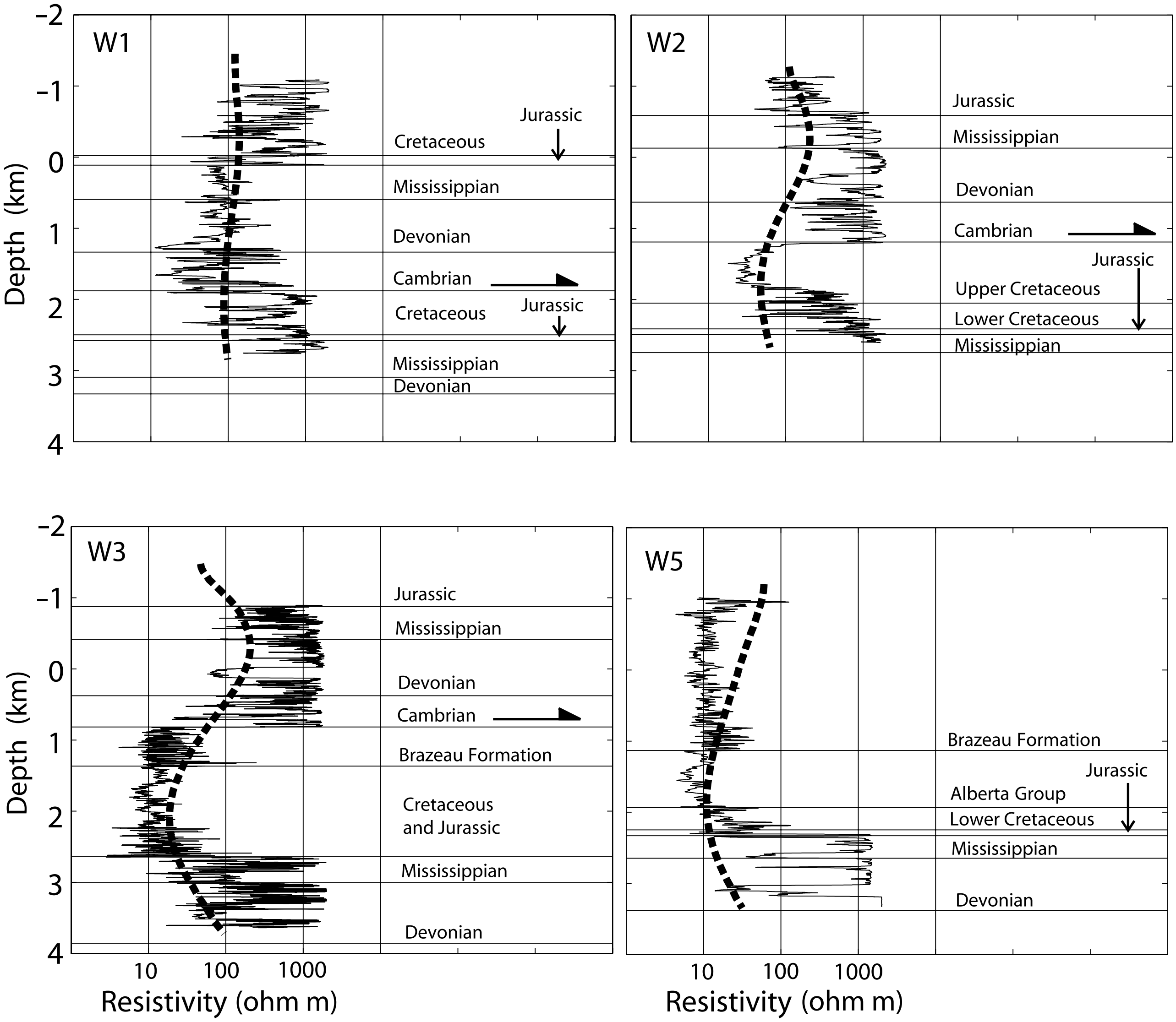

Figure 7. Comparison of resistivity logs (solid lines) and the magnetotelluric derived resistivity model (dashed lines) at four wells. The depth is relative to sea level, and well locations are shown in Figure 3. W1 = 00/06-32-035-12w500, W2 = 00/11-02-036-12w500, W3 = 00/05-13-037-12w500, W5 = 00/10-16-037-10w500.

The low resistivity of the Cretaceous units provides a major property contrast and allows them to be imaged with magnetotelluric data. This low resistivity value is primarily caused by the porosity and pore-fluid salinity. Brine with a total dissolved solid value of 300 g/L has a resistivity value of 0.2 ohm m (Block, 2001). The gross porosity of the strata can be estimated from its resistivity by Archie's (1942) law. Using a salinity of 300 g/L and a bulk resistivity of 10 ohm m for the Cretaceous section from the magnetotelluric inversion model, an overall porosity of 22–28% can be estimated, with cementation factors of $m = 1$ and 2. It should also be noted that the resistivity may be decreased by clay conduction in shale units (Waxman and Smits, 1968).

Triangle Zone

A triangle zone can be observed in the seismic section between the distances of 20 and 40 km (12 and 24 mi) (Figure 4a), with the basal detachment inferred to be at the base of the Brazeau Formation. Shortening above the detachment has caused the formation of two anticlines (A1 and A2) and a syncline (S) east of the Brazeau thrust fault. In the inversion model (Figure 4b), the low-resistivity layer A can be traced west into the footwall of the Brazeau thrust fault. The hanging wall comprises at least 1700 m (5577 ft) of high-resistivity Paleozoic strata. The uplift of the low-resistivity layer east of the Brazeau thrust fault

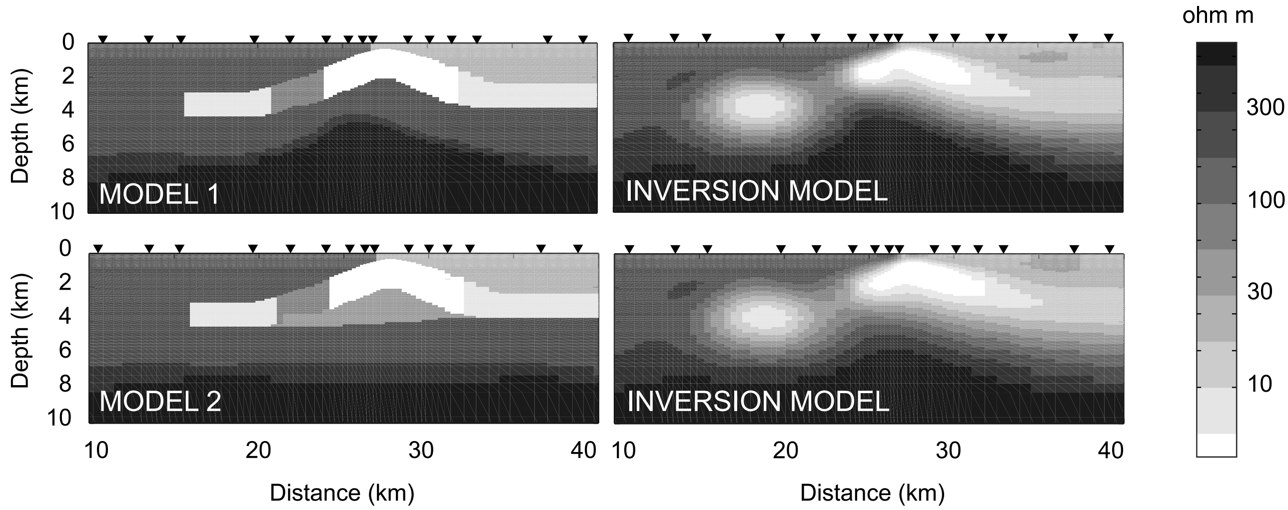

Figure 8. Synthetic inversion test to examine model sensitivity below the low-resistivity anticline A1 (Figure 4b). Models 1 and 2 were generated with different values of resistivity beneath the anticline (A1). Synthetic data were then generated for each model, and 5% Gaussian noise was added to these data. The synthetic magnetotelluric data were then inverted using the same algorithm and parameters as for the field data. The final root-mean-square (rms) misfits are as follows: model 1, rms = 0.88; model 2, rms = 0.90. The models show that resolution of the model below the anticline A1 is poor.

is interpreted as the anticline A1, which reaches the surface at a distance of 28–29 km (17–18 mi). The high-resistivity gap (feature D) is required by the magnetotelluric data (Xiao, 2004) and is interpreted as a syncline. The small uplift of the low-resistivity layer east of S is interpreted as the anticline A2. The geometry of these four resistivity features is consistent with the geometry imaged in the seismic section.

The pronounced resistivity change between the anticline and syncline could be explained by changes in fracture permeability in the Cretaceous strata. Tension or compression will increase or decrease the permeability of the strata at the axis, respectively. In the presence of low-resistivity (saline) groundwater, this will lower the electrical resistivity in the anticline and increase it in the synclines, as observed (assuming a relatively uniform distribution of groundwater in the formation). This phenomena has been observed in other magnetotelluric surveys (Orange, 1989) and allows magnetotelluric data to remotely sense fracture permeability in reservoir rocks.

An apparent uplift of the high-resistivity basement is observed below A1 in the inversion model (U in Figure 4b). This does not agree with the seismic data because in the seismic section, the strata at this location are subhorizontal. To evaluate if feature U is required by the magnetotelluric data, a synthetic inversion was undertaken (Figure 8). In this procedure, several models are constructed based on Figure 4b. The magnetotelluric data predicted for these models were then computed, and 5% noise was added. These data were then inverted using the same algorithm that was applied to the real magnetotelluric data. Models with resistivity values of 30 and 300 ohm m below A1 both give the same inversion result. Thus, the model containing feature U is not the only one that fits the magnetotelluric data. A model with a flat base for the Mesozoic and Paleozoic strata is also consistent with the magnetotelluric data. This study showed that beneath the low-resistivity anticline A1, the resolution of the model is poor.

Underthrust Cretaceous Rocks

To the west, the Brazeau thrust fault is characterized by a high-resistivity hanging wall (10–25 km; 6–15 mi) with the low-resistivity footwall that dips westward at approximately 30°. The resistivity of the footwall is not uniform, and a high-resistivity gap (50–70 ohm m) is observed at a distance of 21–24 km (13–14 mi) (B). The footwall units exhibit a low-resistivity zone again west of feature B at a distance of 21–14 km (13–8 mi) (C). Farther west, the footwall resistivity increases again to above 100 ohm m (E).

The high-resistivity feature B observed in the inversion model could be caused by a decrease in porosity and permeability or a decrease of the formation fluid salinity. A porosity and permeability decrease could result from lithological changes or the increased compaction with depth. The escape of high-salinity

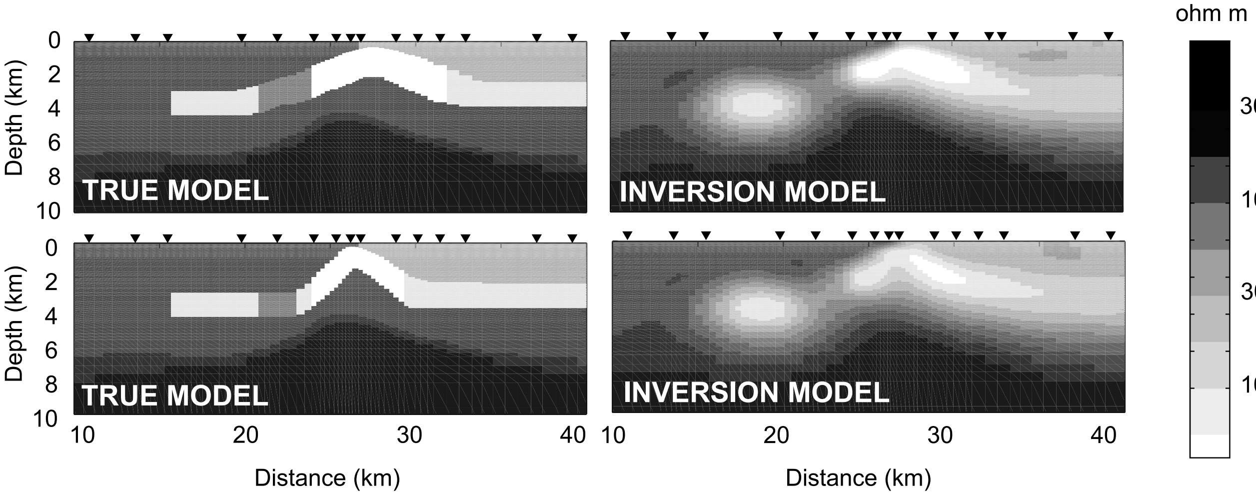

Figure 9. Synthetic inversion test to examine sensitivity of the dip angle of the Brazeau thrust fault to the measured magnetotelluric data. Left: synthetic resistivity models with dips of 30° and 45°, top and bottom, respectively; right: inversion results. Final root-mean-square misfits are 0.88 (30° model) and 0.99 (45° model). The results show that these two models can easily be distinguished with the survey geometry used in the actual survey.

formation fluid during thrusting or mixing with meteoric water could also decrease the formation fluid salinity and, thus, increase the overall formation resistivity. In this interpretation, the top of feature C corresponds to the Brazeau thrust fault, and the base is coincident with the base of the Cretaceous section. If a value of 10 ohm m is used to identify these boundaries, then the top is at a depth of about 2400 m (7874 ft), and the base is at 4500 m (14,763 ft). From well-log W3 (Figure 7), the Cretaceous strata lie between the depths of 2313 and 4065 m (7588 and 13,336 ft). Thus, the depths determined from the magnetotelluric model are within 10% of those observed in the well logs. The well-log and seismic data suggest that B, C, and E are all located within Cretaceous strata. Well-log W1 (Figure 7) showed that the resistivity of the Cretaceous strata at this location is quite high and in agreement with feature E (Figure 4b). Note that the low-resistivity feature C is obvious in well-logs W3 and W2. Well-log W3 shows a good agreement between the magnetotelluric model and the resistivity log data. The decrease of resistivity in C could be caused by enhanced porosity associated with the transition from ramp to flat on the Brazeau thrust fault. Possible reasons for the resistivity increase in region E could be a decrease in permeability and/or porosity caused by lithological change or the escape of high-salinity pore fluids.

A synthetic inversion was used to investigate how reliably the magnetotelluric data can determine the dip of the Brazeau thrust fault. The synthetic models (Figure 9) have the same resistivity structure except for the dip angle of the Brazeau thrust fault. The inversion results show that the magnetotelluric data are sensitive to the dip angle, and that it is well constrained at approximately 30°.

CONCLUSIONS

This study has shown that the geometries of the major resistivity structures derived from the magnetotelluric data are in reasonable agreement with the coincident seismic reflection and well-log data. This suggests that structural imaging in the Rocky Mountain Foothills is feasible with magnetotelluric exploration. Although the resolution of magnetotelluric exploration is lower than that of seismic exploration, the lower cost and reduced environmental impact represent advantages as a reconnaissance tool in exploration.

The resistivity model can potentially provide information about the structure and composition of hydrocarbon reservoirs because porosities can be estimated from resistivities using Archie's law. This has the potential to allow the detection of fracture-related porosity changes around the hinges of anticlines and synclines.

Like any geophysical method, magnetotellurics requires a contrast in material properties to image structures. In the study area, the low-resistivity Cretaceous section provides a major contrast in resistivity with the high-resistivity Paleozoic thrust sheet. In other locations, this might not be the case. However, underthrust clastic rocks are commonly lower in resistivity than overthrust carbonates or older units as demonstrated in other magnetotelluric studies of similar tectonic settings. When combined with seismic data, the modern magnetotelluric method has the potential to yield useful information about the geometry of thrust sheets and a way of determining the degree of fracture-related permeability.

APPENDIX: ACQUISITION COSTS FOR MAGNETOTELLURIC DATA

Magnetotelluric data are routinely collected by several commercial contractors. For a 100-station magnetotelluric survey in terrain such as the Foothills, the cost per station quoted by two leading contractors is in the range of US $1000–2000. This assumes relatively simple ground-based logistics and does not include mobilization or demobilization. Survey time is controlled by the number of instruments used. For example, with five recording units and overnight recording at all stations, this would require a minimum survey time of 20 days. Basic processing of the data is typically priced at US $250+ per station. However, the advanced processing needed for detailed analysis and interpretation would require 1–2 weeks of work by a geophysicist experienced with magnetotellurics.

REFERENCES CITED

Archie, G. E., 1942, The electric resistivity log as an aid in determining some reservoir characteristics: Transactions of the American Institute of Mining, Metallurgical and Petroleum Engineers, v. 146, p. 54–62.

Bedrosian, P. A., M. J. Unsworth, and F. Wang, 2001, Structure of the Altyn Tagh fault and Daxue Shan from magnetotelluric surveys: Implications for faulting associated with the rise of the Tibetan Plateau: Tectonics, v. 20, p. 474–486.

Block, D., 2001, Water resistivity atlas of Western Canada abstract: http://www.cspgconvention.org/archives/2001abstracts/P-088.pdf (accessed July 20, 2005).

Cagniard, L., 1953, Basic theory of the magnetotelluric method of geophysical prospecting: Geophysics, v. 18, p. 605–635.

Christopherson, K. R., 1991, Applications of magnetotellurics to petroleum exploration in Papua New Guinea— A model for frontier areas: The Leading Edge of Exploration, April, v. 10, no. 4, p. 21–27.

deGroot-Hedlin, C., 1991, Removal of static shift in two dimensions by regularized inversion: Geophysics, v. 56, p. 2102–2136.

Densmore, A. A., 1970, An interpretation of some magnetotelluric data recorded in northeast British Columbia during 1969: Journal of the Canadian Society of Exploration Geophysicists, v. 6, p. 34–38.

Duckworth, K., 1983, Electrical surveys in the Alberta Foothills: Journal of the Canadian Society of Exploration Geophysicists, v. 19, p. 57–66

Egbert, G. D., 1997, Robust multiple-station magnetotelluric data processing: Geophysical Journal International, v. 130, p. 475–496.

Gamble, T. D., W. M. Goubau, and J. Clark, 1979, Magnetotelluric with a remote magnetic reference: Geophysics, v. 44, p. 53–68.

Jones, A., 1988, Static shift of MT data and its removal in a sedimentary basin environment: Geophysics, v. 53, p. 967–978.

Jones, A. G., and H. Jodicke, 1984, Magnetotelluric transfer function estimation improvement by a coherence-based rejection technique: 54th Annual International Meeting, Society of Exploration Geophysicists, Atlanta, Georgia, U.S.A.: p. 51–55.

Jones, P. B., 1982, Oil and gas beneath east-dipping underthrust faults in the Alberta Foothills, *in* R. B. Powers, ed., Studies of the Cordilleran thrust belt: Rocky Mountain Association of Geologists, p. 61–74.

Langenberg, C. W., A. Beaton, and H. Berhane, 2002, Regional evaluation of the coalbed methane potential of the foothills/mountains of Alberta, 2d ed.: Energy and Utility Board/Alberta Geological Survey Earth Science Report 2002-05, 90 p.

Lawton, D. C., C. Sukaramongkol, and D. A. Spratt, 1996, Seismic characterization of a compound tectonic wedge beneath the Rocky Mountain foreland basin, Alberta: Bulletin of Canadian Petroleum Geology, v. 44, p. 258–268.

Mackie, R. L., T. R. Madden, and P. E. Wannamaker, 1993, Three-dimensional magnetotelluric modeling using difference equations— Theory and comparisons to integral equation solutions: Geophysics, v. 58, p. 215–226.

McNeice, G. W., and A. G. Jones, 2001, Multisite, multifrequency tensor decomposition of magnetotelluric data: Geophysics, v. 66, p. 158–173.

Monger, J. W. H., and R. A. Price, 1979, Geodynamic evolution of the Canadian Cordillera— Progress and problems: Canadian Journal of Earth Sciences, v. 16, p. 770–791.

Orange, A. S., 1989, Magnetotelluric exploration for hydrocarbons: Proceedings of the Institute of Electrical and Electronics Engineers, v. 77, p. 287–317.

Park, S. K., S. C. Thompson, A. Rybin, V. Batalev, and R. Bielinski, 2003, Structural constraints in neotectonic studies of thrust faults from the magnetotelluric method, Kochkor Bain, Kyrgyz Republic: Tectonics, v. 22, p. 1013–1025.

Rodi, W., and R. Mackie, 2001, Nonlinear conjugate gradient algorithm for two-dimensional magnetotelluric inversion: Geophysics, v. 66, p. 174–187.

Simpson, F., and K. Bahr, 2004, Practical magnetotellurics: Cambridge, Cambridge University Press, 250 p.

Sternberg, B. K., J. Washburne, and L. Pellerin, 1988, Correction for the static shift in MT using transient electromagnetic soundings: Geophysics, v. 53, p. 1459–1468.

Tikhonov, A. N., 1950, Determination of the electrical characteristics of the deep strata of the Earth's crust: Doklady Akademii Nauk (Proceedings of the Russian Academy of Sciences), v. 73, no. 2, p. 295–297.

Torres-Verdin, C., and F. X. Bostick, 1992, Principles of spatial surface electric field filtering in magnetotellurics— Electromagnetic array profiling (EMAP): Geophysics, v. 57, p. 603–622.

Vozoff, K., 1991, The magnetotelluric method, *in* J. D, Corbett, ed., Electromagnetic method in applied geophysics— Applications part A and part B: Society of Exploration Geophysicists, p. 641–711.

Watts, M., and A. Pince, 1998, Petroleum exploration in overthrust areas using magnetotelluric and seismic data: Society of Exploration Geophysicists, Expanded Abstracts 68th Annual International Meeting, p. 429–431.

Waxman, M. H., and L. J. M. Smits, 1968, Electrical conductivities in oil-bearing shaly sands: Society of Petroleum Engineers Journal, v. 243, p. 107–122.

Wright, G. N., M. E. McMechanm, and D. E. G. Potter, 1994, Structure and architecture of the Western Canada sedimentary basin, *in* G. D. Mossop and I. Shetsen, compilers, Geological atlas of the Western Canada sedimentary basin: Calgary, Canadian Society of Petroleum Geologists and the Alberta Research Council, p. 25–40.

Xiao, W., 2004, Magnetotelluric exploration in the Rocky Mountain Foothills: Master's thesis, University of Alberta, Edmonton, Alberta, Canada, 97 p.